ELSEVIER

European Journal of Cancer 41 (2005) 799–806

European Journal of Cancer

www.ejconline.com

Tumour parameters affected by combretastatin A-4 phosphate therapy in a human colorectal xenograft model in nude mice☆

Ethaar El-Emir *, Geoffrey M. Boxer, Ingrid A. Petrie, Robert W. Boden, Jason L.J. Dearling, Richard H.J. Begent, R. Barbara Pedley

Cancer Research UK Targeting and Imaging Group, Department of Oncology, Royal Free and University College Medical School, Rowland Hill Street, London NW3 2PF, UK

Received 20 August 2004; received in revised form 24 November 2004; accepted 4 January 2005

Abstract

Combretastatin A-4 phosphate (CA4-P) is an antivascular agent which inhibits tumour blood flow. The effects of CA4-P were studied at 1 and 24 h in colorectal xenografts by the concomitant imaging of multiple physiological parameters (hypoxia, blood vessels and perfusion), selected to demonstrate changes related to vascular shut-down. Untreated tumours were viable, with perfused blood vessels throughout and only small areas of hypoxia. At 1 h post-treatment, although blood vessels remained throughout the tumour, perfused vessels were mainly restricted to the rim. However, hypoxia was widespread in both peripheral and central parts of the tumour. Quantitative analysis also revealed a significant decrease in perfusion and a maximum increase in hypoxia at this time-point. Conversely, at 24 h after treatment, when most of the tumour was necrotic, pathophysiological conditions in the surviving viable rim were already returning to normal: perfusion was increasing, and hypoxia was greatly reduced and restricted to regions bordering central necrosis. In conclusion, these data provide an insight into the actions by which CA4-P may exert its effects on solid tumours.

Keywords: Combretastatin A-4; Xenograft; Colorectal; Mice; Tumour parameter; Hypoxia; Vasculature; Perfusion

1. Introduction

It is widely accepted that tumour vasculature is critical for both the survival and the continuous growth of tumours [1,2]. It also determines the type of microenvironment that exists within a tumour and thus influences tumour response to therapy [3]. These findings have led to a significant research effort to develop therapies that specifically target and damage tumour vasculature, either by inhibiting its development (anti-angiogenic therapy) or specifically destroying established vessels (anti-vascular therapy) [4]. Vascular targeting aims to exploit the differences between tumour and normal vasculature by irreversibly arresting tumour blood flow and producing tumour cell death by oxygen and nutrient starvation. However, although there is some understanding of the effects of anti-vascular agents on tumour endothelial cells, much less is known about their overall effects on the tumour as a whole. As tumour microenvironment is a key factor in tumour biology and has a large impact on response to treatment, analysis of multiple tumour parameters is essential in order to obtain a better understanding of the modes of action of anti-vascular agents, thereby optimising therapy.

Two main classes of drugs have been identified as having anti-vascular activity [5]. First, compounds related to

☆ This work is supported by the International Association for Cancer Research, Cancer Research UK and the European Union FP6 Grant, LSCH-CT-2003-503233, STROMA.
* Corresponding author. Tel.: +44 2077940500x1453/5496; fax: +44 2077943341.
E-mail address: e.el-emir@ucl.ac.uk (E. El-Emir).

0959-8049/$ - see front matter © 2005 Elsevier Ltd. All rights reserved.
doi:10.1016/j.ejca.2005.01.001

flavone acetic acid which are thought to cause vascular injury via the tumour necrosis factor-α pathway, for example 5,6-dimethyl-xanthenone-4 acetic acid (DMXAA) [6–8]. Second, the tubulin binding agents, which include combretastatin A-4 phosphate (CA4-P) [9,10].

CA4-P is a compound originally isolated from *Combretum caffrum*, a southern African shrub [11]. In contrast to colchicines and other tubulin-binding agents that have been investigated for disrupting tumour vasculature and for which there is significant dose-limiting toxicity, CA4-P is active at one-tenth of the maximum tolerated dose, offering a wide therapeutic window [12]. The precise mechanism of action of CA4-P is not fully understood, but it has been shown to specifically target dividing endothelial cells and block mitosis through binding to tubulin, causing destabilisation of the cytoskeleton [12]. *In vivo*, CA4-P has been shown to cause rapid reduction in tumour blood flow followed by large-scale central necrosis in a range of animal and human xenografts [12–15], as well as in spontaneous animal tumours [16]. In addition, it has also been shown to enhance outcome when used in combined therapies such as radiation and chemotherapy [17], hyperthermia [18] and antibody-based approaches [19,20]. Furthermore, in Phase I clinical trials, a single dose of CA4-P was shown to cause changes consistent with tumour blood flow reduction [21]. This drug is currently entering a range of combined-therapy trials, including antibody-targeted treatment for colorectal cancer [19].

The aim of the present study was to investigate, within the same whole tumour section, the effects of CA4-P on selected tumour parameters at different time-points using a human colorectal xenograft (SW1222) in nude mice. These include morphology, blood vessel distribution, vascular perfusion and hypoxia. Furthermore, we show quantitative data of the changing relationship between the latter three parameters at a microscopic level following CA4-P treatment. This is the first time that these techniques have been used to investigate the effects of anti-vascular drugs on tumour biology over time.

In this study, we demonstrate how quantitative microscopy can be used to investigate relative changes in a range of tumour parameters within the same whole tumour section following anti-vascular therapy. This same technique can be used to study the therapeutic effects of any cancer treatment and will allow the optimisation of both type and timing of therapy.

2. Materials and methods

2.1. Tumours and drug treatment

The human colorectal adenocarcinoma SW1222 was grown as subcutaneous (s.c.) xenografts in the flanks of nude mice [19]. Tumours were selected for treatment when they reached approximately 1 cm in diameter, 10–14 days after implantation. All experiments were in compliance with the United Kingdom (UK) Coordinating Committee on Cancer Research Guidelines for the Welfare of Animals in Experimental Neoplasia.

CA4-P, supplied by OXiGENE, was made up in sterile normal saline immediately prior to use. Two groups of 3 mice each were injected with a single dose (200 mg/kg) of CA4-P and sacrificed at 1 and 24 h post-treatment. A further group of 3 mice who were not given any drug was used as controls. Tumours were removed, snap-frozen in isopentane (cooled over liquid nitrogen), sectioned at 10 μm and stored at −80 °C.

2.2. Tumour parameters

The effect of CA4-P on selected tumour parameters was studied in detail using the following markers:

1. *Perfusion*. Hoechst 33342 (Molecular Probes) was injected intravenously (i.v.) at a concentration of 10 mg/kg 1 min before sacrifice. This marker is viewed directly under an ultraviolet (UV) filter.
2. *Hypoxia*. Mice were injected with 60 mg/kg pimonidazole intraperitoneally (i.p.) 30 min before sacrifice and a fluorescein isothiocyanate (FITC)-conjugated anti-pimonidazole antibody was used to identify hypoxic areas within the tumour.
3. *Tumour vasculature*. An anti-CD31 antibody and an Alexa Fluor 546 conjugated secondary antibody were used to detect blood vessel distribution within the tumour.
4. *Morphology*. Haematoxylin and eosin (H&E) staining of the same section was carried out in order to compare the distribution of fluorescence with tumour structure/architecture.

2.3. Fluorescence immunohistochemistry

After thawing, sections were fixed in acetone for 10 min and left to air dry at room temperature. Sections were then blocked in 3% normal goat serum and incubated with a 1:2 dilution of unconjugated anti-CD31 rat anti-mouse (A kind gift from Professor A. Mantovani) for 1 h at room temperature. After rinsing in phosphate-buffered solution (PBS), sections were incubated simultaneously with a 1:200 dilution of Alexa Fluor 546 goat anti-rat antibody (Molecular Probes), and with a 1:2000 dilution of a FITC-conjugated rabbit polyclonal anti-pimonidazole antibody (A kind gift from Professor J. Raleigh). After rinsing in PBS, sections were mounted in PBS and viewed under a fluorescence microscope (see below).

2.4. Fluorescence image generation and quantification

Sections were viewed on an Axioskop 2 microscope (Zeiss, UK), (at 200× magnification), fitted with a computer-controlled motorised stage, and the images captured by an AxioCam digital colour camera using KS300 image analysis software (Zeiss, UK) [20].

Each tumour section was placed on the motorised stage and then scanned for all three fluorescence parameters, using the appropriate filter for each of the markers. Perfusion was viewed by a UV filter (365 nm excitation), hypoxia by a FITC filter (450–490 nm excitation), and blood vessel distribution by a rhodamine filter (546 nm excitation). A threshold value, equivalent to the exposure in milliseconds, was used to distinguish the signal from background and was determined for each individual marker before the scanning process. After each scan, which consisted of a large number of individual fields (225–400), a composite tiled image was reconstructed for each marker. When scanning of all three fluorescent markers was complete, the same tumour section was then stained with H&E and scanned under bright field microscopy. The whole scanning procedure therefore yielded four composite images for each tumour section showing perfusion (Hoechst 33324), hypoxia (pimonidazole), blood vessel distribution (CD31) and morphology (H&E). The fluorescence images were then co-registered using Adobe Photoshop software, resulting in a new multichannel image showing overlapping fluorescently labelled structures. In order to quantify the changing relationship of the tumour parameters following therapy, regions of interest (ROI) within the tumour were defined by manually drawing on the corresponding H&E image, demarcating regions of viable tumour tissue and excluding those necrotic and non-tumour areas. The number of pixels in the ROI (i.e., viable tissue) was then calculated as a percentage of the whole tumour section. Finally, the relative intensity for each fluorescent marker in each pixel was measured using an Interactive Data Language (IDL) program (IDL, UK), the latter representing the corresponding parameter fraction within the ROI.

3. Results

In order to assess and quantify the extent of damage produced by CA4-P, sections from both control and treated tumours underwent both fluorescence and H&E staining, and image analysis.

3.1. Regional distribution of parameters following CA4-P treatment

3.1.1. Untreated tumours

Morphology. H&E staining revealed the typical histological appearance of SW1222 tumours, showing them to be moderately differentiated with malignant glandular acini supported by connective tissue stroma. The tumour was mainly viable with only limited necrosis (Fig. 1(e)).

Vasculature, perfusion and hypoxia. Simultaneous demonstration of both CD31 and Hoechst revealed perfused blood vessels throughout both central and peripheral areas of the tumour (Fig. 1(a) and (b)). In contrast, pimonidazole staining demonstrated only small areas of hypoxia within the tumour (Fig. 1(c)). These areas tended to be distant from blood vessels (Fig. 1(f)) and/or bordering areas of tumour necrosis. Fig. 1(d) shows a co-registered image of the three fluorescence parameters across the same tumour section.

3.1.2. CA4-P-treated tumours

The effects of CA4-P on tumour parameters were assessed in SW1222 tumours at 1 and 24 h after treatment.

3.1.2.1. 1 h post-treatment. Morphology. H&E staining revealed that, after a 1-h treatment with CA4-P, treated tumours retained a similar morphology to untreated tumours. At this time-point, most of the tumour appeared viable with some areas of haemorrhage and necrosis (Fig. 2(a)).

Vasculature, perfusion and hypoxia. In spite of the lack of morphological change at this time-point, the functional biology of the tumour was drastically altered. Treatment with a single i.p. dose of 200 mg kg^{-1} of CA4-P resulted in almost complete vascular shutdown in SW1222 tumours 1 h after treatment as demonstrated by Hoechst staining (Fig. 2(b)). Co-registration of fluorescence staining for both Hoechst and CD31 revealed that, although blood vessels were still distributed throughout the whole of the tumour, perfusion was now predominantly confined to the outer rim of fibrous connective tissue capsule surrounding the tumour. The occasional perfused blood vessels found within the tumour region itself were mainly seen at the tumour edge (Fig. 2(b)). By contrast, pimonidazole staining, revealed that at this time-point large areas of hypoxia had developed throughout the tumour (Fig. 2(b)). These were found in both central and peripheral regions of the tumour, primarily adjacent to non-perfused blood vessels (Fig. 2(c)). However, some hypoxia also developed at a distance from perfused blood vessels and surrounding regions of necrosis.

3.1.2.2. 24 h post-treatment. Morphology. At 24 h following CA4-P treatment, the centre of the tumour was necrotic with only a peripheral rim of viable cells remaining as demonstrated by H&E staining (Fig. 2(d)).

Vasculature, perfusion and hypoxia. Fluorescence staining showed that both perfusion and blood vessel

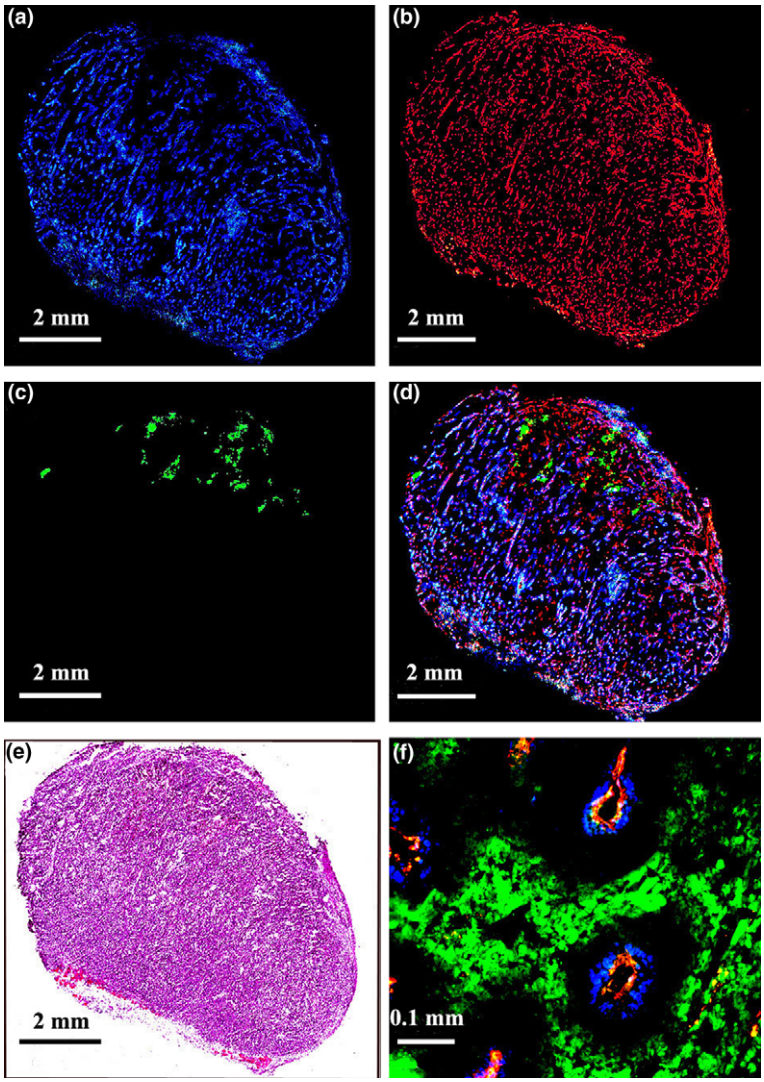

Fig. 1. Fluorescence microscopy of a control untreated tumour stained by triple immunofluorescence as described in the text. (a)–(e) Composite images of the same tumour section showing (a) perfusion (Hoechst 33342), (b) blood vessel distribution (anti-CD31), (c) hypoxia (pimonidazole), (d) a co-registered image of all three parameters and (e) H&E staining of the same tumour section demonstrating morphology. (f) Detail of the untreated tumour demonstrating the development of hypoxia (green) at a distance from perfused (blue) blood vessels (red). All images at 200× magnification.

distribution were restricted to this viable region at the edge of the tumour, although remnants of blood vessels were also found in the more central necrotic areas (Fig. 2(e)). Furthermore, some areas of pimonidazole staining were also seen in the viable rim, demonstrating hypoxic cells bordering regions of tumour necrosis (Fig. 2(e)).

3.2. Quantification of the different parameters following CA4-P treatment

Quantitative analysis of the fraction of viable tissue within the whole tumour section following CA4-P treatment was first carried out (Fig. 3). The percentage of viable tissue was similar for both untreated and 1 h-treated tumours (78% and 73%, respectively). However, at 24 h after treatment, this fraction was significantly reduced to 16% (Fig. 3).

Next, quantitative analysis of the relationship between the different tumour parameters in viable tissue (i.e. ROI) was carried out to demonstrate their relative changes over time following CA4-P treatment (Fig. 4). In untreated tumours, blood vessel distribution occurred at a frequency of 7.9%. After treatment, this fraction rapidly declined to 4.3% by 1 h and subsequently remained at this level, being only 4.8% at 24 h following CA4-P treatment. Perfusion also occurred at a maximum frequency measuring 12.3% in the untreated tumours. After therapy, this proportion was markedly reduced to 1.5% at 1 h, but had risen to 3.4% at 24 h following treatment. By contrast, hypoxia measured 1.7% in the control tumours. At 1 h post-treatment, there was a significant increase in the fraction of hypoxia to a maximum of 23.7%, followed by a return to control levels (1.4%) at 24 h post-treatment.

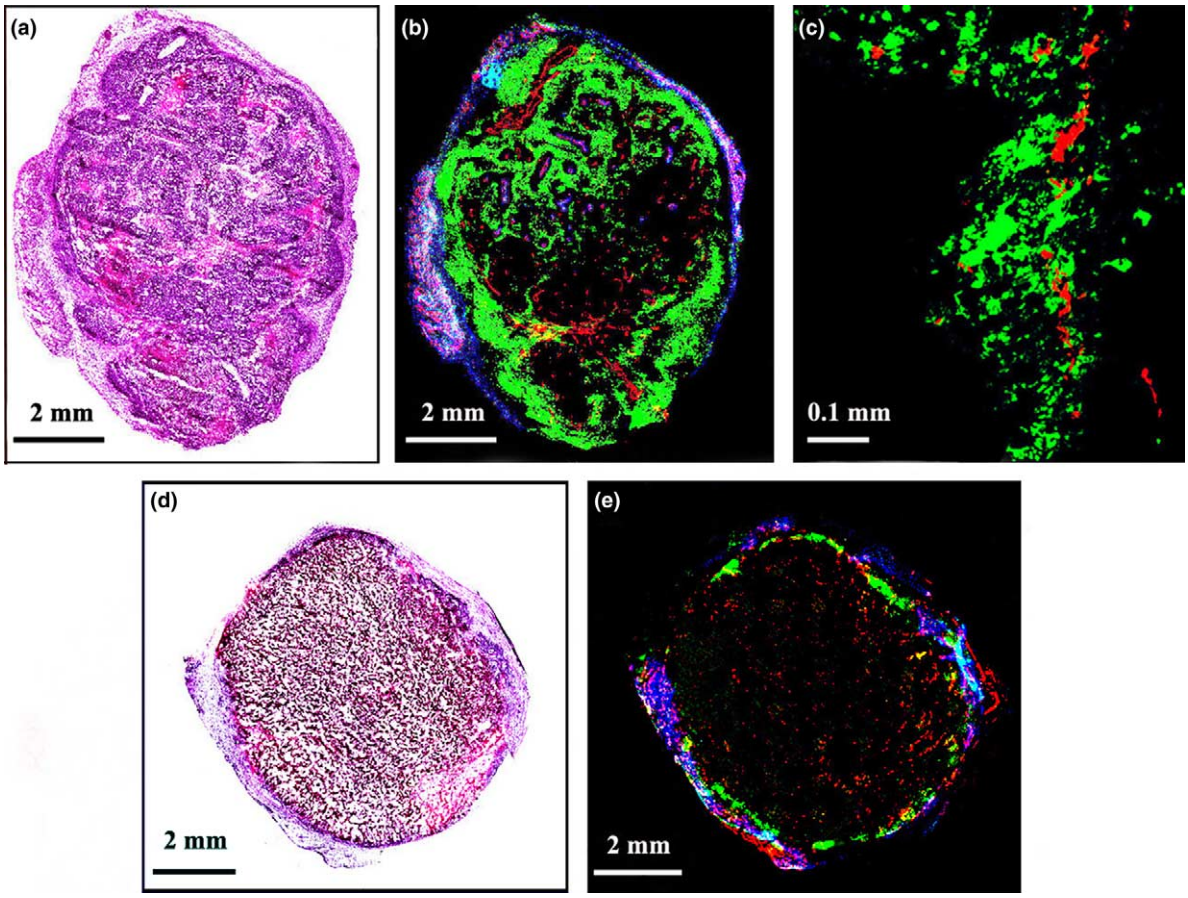

Fig. 2. Effects of CA4-P at 1 (a)–(c) and 24 (d)–(e) hours. (a) An H&E composite image of a 1-h treated tumour section demonstrating tumour morphology, (b) a corresponding co-registered composite image of the same tumour section showing all three parameters: Perfusion (blue), hypoxia (green) and blood vessel staining (red). (c) Detail of the 1 h-treated tumour demonstrating the development of hypoxia (green) adjacent to non-perfused blood vessels (red). (d) An H&E composite image of a 24-h treated tumour section demonstrating tumour morphology, and (e) a corresponding co-registered composite image of the same tumour section showing all three parameters: Perfusion (blue), hypoxia (green) and blood vessel staining (red). All images at 200× magnification.

4. Discussion

This study provides further insight into the effects of CA4-P on solid tumours. We have shown microscopically that CA4-P specifically causes alterations in patterns of vascular distribution, perfusion and the state of hypoxia in SW1222 tumours over time. Furthermore, we provide quantification data for the changes in these parameters following CA4-P treatment. By using quantitative analysis of the changes in spatial relationships between three different fluorescent markers simultaneously, we have dissected the tumour parameters affected by CA4-P at both early and late time-points. Furthermore, by studying two time-points following administration, we have generated additional information about the temporal effects of the drug on tumours.

Untreated tumours were highly vascular, with abundant perfusion and very little hypoxia. At 1 h after treatment, CD31 staining still revealed that blood vessels were distributed throughout the tumour. However, combination with the Hoechst marker demonstrated that perfused vessels were now limited to the edge of the tumour, with only a few found in the centre. Conversely, hypoxia could now be seen throughout the whole of the tumour, both in peripheral and central regions as demonstrated by pimonidazole staining. This pattern of distribution was further confirmed by glut-1 staining on an adjacent section (data not shown). The use of quantitative analysis revealed a significant reduction in the percentage of perfusion at this time-point, accompanied by a corresponding increase in the fraction of hypoxia, in comparison with untreated tumours. Interestingly, the fractions of viable tissue within both untreated and treated tumours were comparable at this early time-point, comprising most of the tumour section (Fig. 3). These findings show that alterations in the levels of both perfusion and hypoxia represent an early effect of CA4-P treatment despite little or no evidence of change in tumour morphology. These data confirm and enhance previous studies by ourselves and others

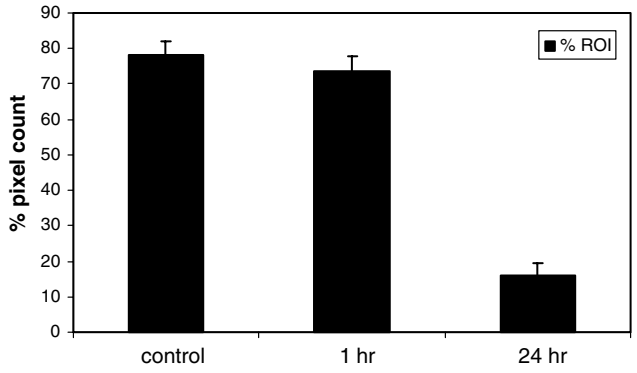

Fig. 3. Histogram showing the percentage of total pixel counts found in viable regions of the tumour over time following CA4-P treatment. The means ± standard error of the means (S.E.M.) of three different tumours are shown. ROI, regions of interest.

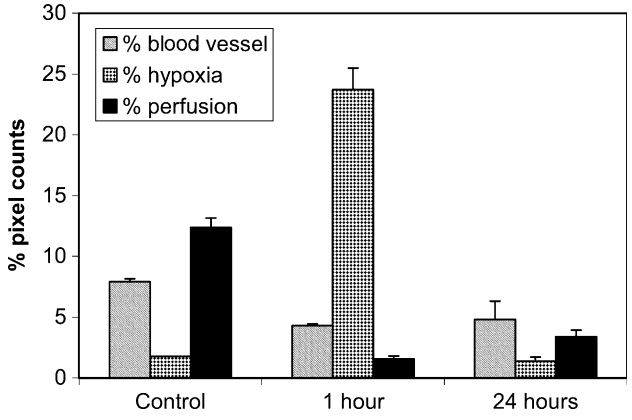

Fig. 4. Histogram showing the quantitative analysis of blood vessel distribution, perfusion and hypoxia over time in CA4-P-treated tumours. The means ± S.E.M. of three different tumours are shown.

showing that, in both single and combined therapy, CA4-P reduces levels of perfusion in a range of tumour models [9,19,22]. In addition, CA4-P has also been shown to increase levels of hypoxia in a number of spontaneous and experimental tumours using oxygen probes [23]. The current study demonstrates that the increase in levels of hypoxia observed at 1 h post-therapy is likely to be a consequence of a rapid block in perfusion caused by CA4-P treatment.

In agreement with several earlier studies [9,19,24], our histological analysis revealed that most of the tumour was necrotic at 24 h post-CA4-P treatment, with only a rim of viable tissue remaining at the periphery. Quantitative data demonstrated that this viable tissue comprised only 16% of the whole tumour section compared with 78% in control and 73% in 1 h-treated tumours (Fig. 3), thus reflecting a significant increase in the amount of necrosis developing by this later time-point. However, within this viable rim of the tumour there was a recovery in perfusion, and a corresponding reduction in hypoxia to control levels, when compared with the 1 h CA4-P treatment (Fig. 4). These data support our previous work with CA4-P which showed that the level of perfusion within the remaining viable rim was significantly reduced at 6 h post-treatment compared with untreated controls, but had started to recover by 24 h after treatment [19]. The increase in perfusion at the rim may relate to a re-perfusion of vessels which had been temporarily shut down by the treatment, or the growth of new vessels. This is important, because the tumour rapidly recommences growth from this remaining peripheral rim of viable cells leading to treatment failure [19,24]. These cells may survive treatment by receiving diffused oxygen and nutrients from adjacent normal host tissue and/or from re-perfused blood vessels within the tumour, which allows their continued proliferation.

CD31 staining demonstrated that blood vessels were distributed throughout the whole tumour in both control and early treatment time-points, but by 24 h they were restricted to the viable rim except for some scattered remnants in the necrotic areas. Furthermore, the quantification data revealed that, although the percentage of blood vessels was reduced following CA4-P treatment, this fraction remained relatively unchanged between 1 and 24 h. This decline in the fraction of blood vessels following treatment may be due to endothelial cell death as a direct consequence of CA4-P treatment. Indeed, a number of *in vitro* studies support this argument. CA4-P has been shown to induce G2/M cell cycle arrest and subsequent death in transformed murine endothelial cells [25]. In addition, CA4-P has been demonstrated to induce apoptotic cell death in human umbilical vein endothelial cells (HUVECs) [26]. More recently, the combretastatin family member, OXI4503, was shown to induce tumour vascular collapse through the induction of endothelial cell apoptosis *in vivo* [27].

This early reduction in the fraction of blood vessels observed in our study (i.e. 1 h after treatment), demonstrates the rapid effects of the drug on tumour endothelium, and the likely subsequent sloughing of endothelial cells. This is interesting in view of the fact that a study using a liver metastatic model demonstrated a significant reduction in the density of blood vessels 1 h after CA4-P treatment [28]. Furthermore, a recent study using CD31 staining in a panel of tumour models demonstrated loss of endothelial cells as early as 2 h following treatment with the tubulin-binding agent ZD6126 [29].

Various reports have demonstrated the effects of the anti-vascular drug CA4-P on single tumour parameters, using a range of techniques. These have included microvasculature using scanning electron microscopy [28], blood flow by magnetic resonance imaging (MRI) [30,31] and hypoxia using computerised fine-needle polarographic oxygen electrode probe [23]; however, this is the first to demonstrate the relative effects of CA4-P on tumour vasculature, perfusion and hypoxia

simultaneously, over time, by fluorescence microscopy. Using these techniques, we have been able to show for the first time that, in spite of the dramatic effects of CA4-P on tumour morphology and pathophysiology, the major parameters determining tumour growth are returning to pre-treatment conditions in the surviving periphery by 24 h after drug administration. This helps to explain why CA4-P is inefficient as a single agent, as it does not inhibit tumour growth, and requires a combined treatment regime in order to realise its full therapeutic potential [18,19].

In the current study, we have described a new approach to the use of montaging techniques for investigating tumour responsiveness to anti-vascular agents. This technique, in which a series of individual microscopic fields is reconstructed using image analysis software to form a composite image of a whole tumour section, was first demonstrated by Rijken and colleagues in Ref. [32], and has since been used to visualise and quantify multiple tumour parameters in various studies [33–35]. In those studies, an adjacent section is generally used to delineate tumour tissue, by excluding non-tumour tissue and necrotic areas. However, in the current study, an H&E image of the same tumour section is used to select the ROI within the tumour in order to carry out the quantification analysis. This has the advantage of allowing more accurate quantification, as all the analysis is made on the same tumour section.

In studies utilising image processing techniques prior to image analysis, the exposure for each fluorophore must be adjusted in order to distinguish clearly between signal and background. Variations in the exposure values could therefore influence the calculations for each parameter fraction. It has been suggested that a fixed threshold for each fluorophore should be used to analyse sections from the same study. It was argued that this should be feasible if all sections were stained using the same protocol at the same time [34]; in our experience, this has not been the case, as different sections fluoresce at different intensities, even when stained simultaneously. However, this does not appear to be a problem in the current study, as the mice within each group give highly reproducible results with small SEMs (see Fig. 4). In addition, the strength of this methodology is that all pixels within the ROI for each tumour are counted allowing all of the data for each parameter to be taken into account. Given this level of accuracy, it has been possible to clearly demonstrate the time-dependent effects of CA4-P on the tumour. Furthermore, this methodology allows us to demonstrate not only the difference in distribution of a single parameter following therapy, but also significant changes in the relationship between the three parameters over time. In an attempt to refine the techniques used to quantify the different fluorescent markers, we are currently exploring other methods that enable more rapid acquisition of images which, in turn, will enhance the sensitivity of fluorophore (marker) detection. In addition, we aim to further dissect the tumour environment by studying a range of additional parameters, for example apoptosis and proliferation, which will enhance our understanding of both tumour microenvironment and its regional responsiveness to therapy. Finally, we are currently applying a three-dimensional system, which allows the reconstruction of a tumour from serial tumour sections, in order to further evaluate the damage caused by CA4-P throughout the whole tumour mass. Considering the whole tumour volume instead of a single section should provide new insights regarding the effect of treatment. As diffusion of molecules is a three-dimensional process, and single images do not take into account out of plane effects of treatment within a tumour, a three-dimensional system will address the intratumoral heterogeneity in regional response to therapy. This, in turn, will lead to a more accurate prediction of therapeutic response in the clinic.

In conclusion, this study has demonstrated the importance of both fluorescence imaging and quantitative microscopy in the analysis of tumour microenvironment parameters following treatment with CA4-P. This technique provides information on the architectural patterns which improves our understanding of the tumour micro-environment, and can be applied to a wide range of anti-vascular and other therapeutic agents. This, in turn, will give insight into their modes of action, thereby allowing the optimisation of single and combined therapies for future clinical trials.

Conflict of interest statement

None declared.

References

1. Folkman J, Shing Y. Angiogenesis. *J Biol Chem* 1992, **267**, 10931–10934.
2. Carmeliet P, Jain RK. Angiogenesis in cancer and other diseases. *Nature* 2000, **407**, 249–257.
3. Denekamp J. Inadequate vasculature in solid tumours: consequences for cancer research strategies. *Br J Radiol* 1992, **24**, 111–117.
4. Chaplin DJ, Dougherty GJ. Tumour vasculature as a target for cancer therapy. *Br J Cancer* 1999, **80**(Suppl. 1), 57–64.
5. Siemann DW, Chaplin DJ, Horsman MR. Vascular-targeting therapies for treatment of malignant disease. *Cancer* 2004, **100**, 2491–2499.
6. Pedley RB, Boden JA, Boden R, *et al.* Ablation of colorectal xenografts with combined radioimmunotherapy and tumour blood flow-modifying agents. *Cancer Res* 1996, **56**, 3293–3300.
7. Pedley RB, Sharma SK, Boxer GM, *et al.* Enhancement of antibody-directed enzyme prodrug therapy in colorectal xenografts by an antivascular agent. *Cancer Res* 1999, **59**, 3998–4003.

8. Baguley BC. Antivascular therapy of cancer: DMXAA. *Lancet Oncol* 2003, **4**, 141–148.
9. Tozer GM, Kanthou C, Parkins CS, *et al*. The biology of the combretastatins as tumour vascular targeting agents. *Int J Exp Pathol* 2002, **83**, 21–38.
10. West CM, Price P. Combretastatin A4 phosphate. *Anticancer Drugs* 2004, **15**, 179–187.
11. Pettit GR, Singh SB, Hamel E, *et al*. Isolation and structure of the strong cell growth and tubulin inhibitor combretastatin A-4. *Experientia* 1989, **45**, 209–211.
12. Dark GG, Hill SA, Prise VE, *et al*. Combretastatin A4, an agent that displays potent and selective toxicity toward tumour vasculature. *Cancer Res* 1997, **57**, 1829–1834.
13. Li L, Rojiani A, Siemann D. Targeting the tumour vasculature with combretastatin A-4 disodium phosphate: effects on radiation therapy. *Int J Radiat Oncol Biol Phys* 1998, **42**, 899–903.
14. Tozer GM, Prise VE, Wilson J, *et al*. Combretastatin A-4 phosphate as a tumour vascular-targeting agent: early effects in tumours and normal tissues. *Cancer Res* 1999, **59**, 1626–1634.
15. Galbraith SM, Chaplin DJ, Lee F, *et al*. Effects of combretastatin A-4 phosphate on endothelial cell morphology *in vitro* and relationship to tumour vascular targeting activity *in vivo*. *Anticancer Res* 2001, **21**, 93–102.
16. Horsman MR, Murata R. Combination of vascular targeting agents with thermal or radiation therapy. *Int J Radiat Oncol Biol Phys* 2002, **54**, 1518–1523.
17. Chaplin DJ, Pettit GR, Hill SA. Anti-vascular approaches to solid tumour therapy: evaluation of combretastatin A4 phosphate. *Anticancer Res* 1999, **19**, 189–196.
18. Murata R, Overgaard J, Horsman MR. Combretastatin A-4 disodium phosphate: a vascular targeting agent that improves the anti-tumour effects of hyperthermia, radiation, and mild thermoradiotherapy. *Int J Radiat Oncol Biol Phys* 2001, **51**, 1018–1024.
19. Pedley RB, Hill SA, Boxer GM, *et al*. Eradication of colorectal xenografts by combined radioimmunotherapy and combretastatin A4-phosphate. *Cancer Res* 2001, **61**, 4716–4722.
20. Pedley RB, El-Emir E, Flynn AA, *et al*. Synergy between vascular targeting agents and antibody-directed therapy. *Int J Radiat Oncol Biol Phys* 2002, **54**, 1524–1531.
21. Dowlati A, Robertson K, Cooney M, *et al*. A phase I pharmacokinetic and translational study of the novel vascular targeting agent combretastatin a-4 phosphate on a single-dose intravenous schedule in patients with advanced cancer. *Cancer Res* 2002, **62**, 3408–3416.
22. Grosios K, Holwell SE, McGown AT, *et al*. In vivo and in vitro evaluation of combretastatin A-4 and its sodium phosphate prodrug. *Br J Cancer* 1999, **81**, 1318–1327.
23. Horsman MR, Ehrnrooth E, Ladekarl M, *et al*. The effects of combretastatin A-4 disodium phosphate in a C3H mouse mammary carcinoma and a variety of murine spontaneous tumours. *Int J Radiat Oncol Biol Phys* 1998, **42**, 895–898.
24. Chaplin DJ, Hill SA. The development of combretastatin A4 phosphate as a vascular targeting agent. *Int J Radiat Oncol Biol Phys* 2002, **54**, 1491–1496.
25. Bohle AS, Leuschner I, Kalthoff H, *et al*. Combretastatin A-4 prodrug: a potent inhibitor of malignant hemangioendothelioma cell proliferation. *Int J Cancer* 2000, **87**, 838–843.
26. Iyer S, Chaplin DJ, Rosenthal DS, *et al*. Induction of apoptosis in proliferating human endothelial cells by the tumour-specific antiangiogenesis agent combretastatin A-4. *Cancer Res* 1998, **58**, 4510–4514.
27. Sheng Y, Hua J, Pinney KG, *et al*. Combretastatin family member OXI4503 induces tumor vascular collapse through the induction of endothelial apoptosis. *Int J Cancer* 2004, **111**, 604–610.
28. Malcontenti-Wilson C, Muralidharan V, Skinner S, *et al*. Combretastatin A4 prodrug study of effect on the growth and the microvasculature of colorectal liver metastases in a murine model. *Clin Cancer Res* 2001, **7**, 1052–1060.
29. Blakey DC, Westwood FR, Walker M, *et al*. Antitumour activity of the novel vascular targeting agent ZD6126 in a panel of tumour models. *Clin Cancer Res* 2002, **8**, 1974–1983.
30. Beauregard DA, Pedley RB, Hill SA, *et al*. Differential sensitivity of two adenocarcinoma xenografts to the anti-vascular drugs combretastatin A4 phosphate and 5,6-dimethylxanthenone-4-acetic acid, assessed using MRI and MRS. *NMR Biomed* 2002, **15**, 99–105.
31. Maxwell RJ, Wilson J, Prise VE, *et al*. Evaluation of the antivascular effects of combretastatin in rodent tumours by dynamic contrast enhanced MRI. *NMR Biomed* 2002, **15**, 89–98.
32. Rijkin PF, Bernsen HJ, van der Kogel AJ. Application of an image analysis system to the quantification of tumour perfusion and vascularity in human glioma xenografts. *Microvasc Res* 1995, **50**, 141–153.
33. Bussink J, Kaanders JH, Rijken PF, *et al*. Vascular architecture and microenvironmental parameters in human squamous cell carcinoma xenografts: effects of carbogen and nicotinamide. *Radiother Oncol* 1999, **50**, 173–184.
34. Rijken PF, Bernsen HJ, Peters JP, *et al*. Spatial relationship between hypoxia and the (perfused) vascular network in human glioma xenografts: a quantitative multi-parameter analysis. *Int J Radiat Oncol Biol Phys* 2000, **48**, 571–582.
35. Ljungkvist AS, Bussink J, Rijken PF, *et al*. Vascular architecture, hypoxia, and proliferation in first-generation xenografts of human head-and-neck squamous cell carcinoma. *Int J Radiat Oncol Biol Phys* 2002, **54**, 215–228.